D.Ph.II/MFL/dmh

PH.I/COM-69-21
20.5.1969

To: Members of the Electronics Experiments Committee

From: M. Ferro-Luzzi, J.M. Perreau, T. Ypsilantis - CERN
G. Bizard, Y. Déclais, J. Duchon, J. Séguinot - University of Caen, France
G. Valladas, CEN, Saclay
C. Bricman, I.I.S.N., Bruxelles.

Subject: Proposal to measure the differential cross section of K^-n elastic scattering between ~ 1 and ~ 2 GeV/c.

I. Motivation

The study of the $\bar{K}N$ interaction in the region immediately above 1 GeV/c is pursued at present in the following directions:

1. Bubble chamber studies of all the reaction channels (including elastic scattering) in K^-p collisions. These are performed mainly by the groups of ref. 1. Photographs were taken at momenta ranging from ~ 1.2 to ~ 1.8 GeV/c in steps of ~ 50 MeV/c. The statistical information is of the order of ~ 20 events/μb per momentum interval and for each experiment. The picture taking and the analysis of the events is in progress.

2. Counter measurements of the polarization and of the differential cross section of the K^-p elastic scattering. The experiment has been partly done and is being continued by the group of ref. 2. The momentum region already studied goes from ~ 1.4 to ~ 2.4 GeV/c in steps of 50 MeV/c; the statistics of the measurements is of the order of a few thousand events per momentum interval.

---

1. The CERN-Heidelberg collaboration and the Collège de France - Rutherford Lab.-Saclay collaboration.
2. The CERN-Holland group: C. Daum et al., Nucl. Phys. B6 (1968) 273 and Nucl. Phys. B7 (1968) 19.

3. A counter measurement of the $K^- p \rightarrow \bar{K}^0 n$ partial cross section in small momentum steps (~ 25 MeV/c) throughout the 1 - 3 GeV/c region. The statistical accuracy amounts to ~ 1%. The experiment has been recently completed by the group of ref. 3.

The situation, as viewed on a cross section plot, is summarized in fig. 1. The interpretation of the results, as far as a complete analysis is concerned, is still in a very early stage. The complete partial wave analysis, which is the eventual outcome of these studies, is not yet possible in view of (a) the insufficient accuracy of the data and (b) the lack of information on essential ingredients. The problem consists, in simplified form, in solving the equations connecting the measured quantities (differential cross sections and polarizations) and the partial waves responsible for the observed phenomena. If the behaviour of the partial waves in the momentum range below ~ 1 GeV/c can be taken as representative, then a large quantity of waves is likely to exhibit resonances. Indications for at least 4 or 5 such resonances have already been found in the region from 1.2 to 2.3 GeV/c and preliminary quantum numbers have been attributed[2,4]. However, a complete understanding of all the partial waves depends on information which at present is either poorly determined or not determined at all. Among the latter is the isotopic spin I = 1 elastic scattering, which is what we propose to measure.

The information available from the existing experiments above 1.2 GeV/c is based on the $K^- p$ incident channel and the analysis must necessarily deal with the complication of an I = 0 and I = 1 mixture. To separate and determine each combination, one is usually obliged to

---

3. The CERN-Caen-Saclay group: C. Bricman et al. (to be published).
4. C.G. Wohl, (thesis) UCRL-16288 (1965) and
   C.G. Wohl et al., Phys. Rev. Letters 17 (1966) 107.

recur to assumptions on the behaviour of specific waves and the quantum number of the most important phenomena observed. The treatment of the absorption channel is, from this point of view, facilitated by the existence of channels which, like $K^- p \rightarrow \Lambda \pi^0$, are in a pure isostopic spin state. Thus it is because an enhancement is seen in the partial cross section for $K^- p \rightarrow \Lambda \pi^0$ at $\sim$ 1.5 GeV/c that the resonance $\Sigma(2030)$ has been attributed isospin 1 and not 0. This procedure, plus an appeal to what is already known at lower energies, is the base of most of the knowledge in this region. Clearly the information coming from the pure isospin reactions in the incident channels would solve many, if not all, problems. As far as we are aware, there are no plans in the bubble chamber world for an extensive investigation of $K^- d$ reactions above 1 GeV/c*). Experiments of the $\bar{K}^0 p$ type would, of course, yield the same information, but the technical problems involved are such as to make rather unlikely their execution in a reasonable time.

II. Experiment proposed

The measurements we propose consist of several runs of K^- on deuterium at conveniently spaced momentum intervals so as to make use of the centre of mass energy spread introduced by the Fermi motion of the neutron. The region covered would be from $\sim$ 1.2 to $\sim$ 2.2 GeV/c, with particular emphasis on 1.5 GeV/c which is known to be the seat of interesting phenomena[2,4]. The statistics at each run and the spacing of the runs is a matter of compromise between the precision wanted on the $K^- n$ cross section and what is already known about the other reactions. If we restrict ourselves to the information that exists (or will exist in the near future) on the $\bar{K}N$ channels, then the $K^- p$ differential cross

*) The most ambitious attempt up to date to investigate $K^- d$ interactions in a bubble chamber above 1 GeV/c is that of the "Birmingham-Edinburgh-Glasgow-Imperial College" collaboration. This has consisted of two runs, at 1.44 and 1.64 GeV/c, yielding respectively 3.0 and 1.6 events/μb.

section will be based on a final statistics of ~ 5,000 events per momentum. The counter experiment of ref. 2 gives the K^-p polarization as a function of the production angle with a statistical accuracy comparable to that mentioned above. The statistics on the charge-exchange reaction, $K^-p \rightarrow \bar{K}^0 n$, will eventually grow to ~ 1,000 events per momentum interval of 40 MeV/c.

The statistics on the K^-n elastic scattering necessary to match the above experiments then requires at least a thousand events per momentum. In view of the complete lack of information on this channel, it is somewhat arbitrary to estimate what is the optimum amount of statistics which would be of use in a partial wave analysis. Probably even a relatively small statistics could be effective in removing ambiguities and guiding the trend of the momentum dependence of the $I = 1$ amplitudes. On the other hand, in view of the high spin of the resonances present in the region ($J = 7/2$ is suggested for $\Sigma(2030)$ and $\Lambda(2100)$ from the analyses of ref. 2 and 4), the statistics should allow a meaningful expansion in polynomials of $\cos\theta$ up to the 7th order. In this connection, it is relevant to examine what is known at present on the coefficients of the Legendre polynomial expansions

$$d\sigma/d\Omega = \lambda\!\!\!^{-2} \Sigma A_n P_n (\cos\theta)$$

$$\vec{P}\, d\sigma/d\Omega = \vec{n}\, \lambda\!\!\!^{-2} \Sigma B_n P_n^1 (\cos\theta) .$$

These expansions (discussed in more detail in the analyses of refs. 1-4) yield the coefficients A_n and B_n which are taken by many as the starting information for a partial wave analysis. In the region near 1.5 GeV/c the published values of the 7th order coefficients for $K^-p \rightarrow K^-p$ and $K^-p \rightarrow \bar{K}^0 n$ are those shown in fig. 2. More precise information on these coefficients will be available in the near future, when the experiments of ref. 1 will be completed, but one can already foresee that the situation represented in fig. 2 may well be too complicated to explain without recurring to independent experimental

information. It should be noticed that the A_7 coefficients of the $K^- p \rightarrow \bar{K}^o n$ reaction have been taken as good evidence[4] that the region near 1.5 GeV/c is dominated by the $J = 7/2$ amplitudes (F_{17} and G_{07}) corresponding to $\Sigma(2030)$ and $\Lambda(2100)$*). In this case one obtains:

$$A_7 (K^- p) \propto \underline{\mathrm{Re}} (F_{17} G_{07})$$

$$A_7 (\bar{K}^o n) \propto -\underline{\mathrm{Re}} (F_{17} G_{07})$$

$$B_7 (K^- p) \propto \underline{\mathrm{Im}} (F_{17} G_{07})$$

The curves in fig. 2 show the values for these coefficients expected under the above hypothesis. One can see that the agreement is far from good, even within the present statistical precision. In particular, the discrepancy in $A_7(K^- p)$ cannot be explained without the presence of an important contribution of background amplitudes in both isospins and for both the $J^P = 7/2^+$ and $7/2^-$ waves (the absence of significant coefficients of order higher than 7 excludes the presence of amplitudes with $J > 7/2$). An attractive hypothesis is that the background amplitudes are nearly isospin independent, so as to cancel out in the $\bar{K}^o n$ reaction while adding in the $K^- p$. The polarization coefficient B_7 would then be exempt, for a large part, of the background contribution. This, of course, is a hypothesis that should be tested; the knowledge of the A_7 coefficient for the pure isospin 1 reaction $K^- n \rightarrow K^- n$ would come very handy at this stage. So as to obtain a reasonable precision on this quantity, we estimate that something between 2 and 3 thousand events would be necessary (considering that the very forward angular region cannot be measured for this reaction; see Appendix II).

---

*) Incidentally, it is on this basis that the determination of spin and parity for these two resonances has been made. The Rosenfeld tables give the spin-parity determination as "well-established".

III. Method

The apparatus we intend to use is schematically outlined in fig. 3. The $\check{C}$, S_1, S_2, S_3 system defines and measures the direction of the incident K^-_{in}; C_1, C_2, C_3 before the magnet, C_4, C_5, C_6 after, define the momentum and direction of the scattered kaon, K^-_{out}; the neutron detector (Appendix I) determines the direction of the recoil neutron*). An anticoincidence wrapping (excluding the exit window for K^-_{out}) ensures that no charged product accompanies the reaction. A lead-scintillator sandwich system (not shown in the figure) takes care of anticoinciding the π^o's. (A Monte Carlo calculation of the contamination expected from reactions of the type $K^-n \rightarrow K^-n\pi^o$ gives an upper limit of $\sim 1\%$). Thus one is left with a $K^-_{in}d \rightarrow K^-_{out}n\,(p_s)$ configuration, with the spectator proton (p_s) having an average momentum smaller than ~ 200 MeV/c (as determined by the size of the target which we take as a 4 cm diameter cylinder). In these conditions, a zero-constraint fit can be performed (if the neutron time-of-flight or its scattering on free protons inside the neutron detector could be measured, we could then gain one additional constraint). The limit on the spectator proton momentum makes it very probable that the interaction has taken place on the neutron and not on the proton.

The size of the available magnets and the practical limit on the dimensions of the chambers impose an angular acceptance such that several settings are necessary in order to cover the full range of laboratory angles of the K^-_{out} (Appendix II). Typically, this number is ~ 6. The running time for angular setting depends on the specific form of the differential cross section and the statistical accuracy needed.

---

*) The purpose of the chambers C_7 and C_8, just in front of the neutron detector, is to allow a measurement (either at all or at selected momenta) of the direction of the recoil proton from $K^-d \rightarrow K^-p\,(n_s)$ reactions; the comparison of the known differential cross sections for K^-p elastic scattering[2] with the above measurement obtained when the K^- scatters on the proton of the deuterium provides an excellent built-in check on the overall performance of the apparatus.

We have used the K^-p elastic scattering data existing in the region[2] to estimate the time necessary. Fig. 4 shows a comparison between the K^-p and K^-n elastic scattering at those momenta where this is possible[5]. Assuming that this similarity remains valid throughout the 1 - 2 GeV/c region, in Appendix III we calculate the reaction yield at each magnet setting throughout the region of interest. The efficiency of the neutron counter has been tentatively assumed as 30%, although larger values can be attained by increasing its size (and cost).

From the yields calculated in Appendix III it appears that in a period of 6 PS weeks we would be able to cover, in steps of ~ 150 MeV/c, the entire region from ~ 1 to ~ 2 GeV/c with satisfactory statistics.

The experiment could be done in the m7 beam. We can be ready for a test with a limited part of the equipment by the beginning of 1970. If we are allowed to parasite behind the area which will be occupied by the experiment No. S74 ($\Delta S/\Delta Q$) we could then be ready to run as soon as this group leaves the floor.

---

5. B. Conforto et al., Nucl. Phys. B8 (1968) 265.
   R. Armenteros et al., "The $\bar{K}N$ interaction from 800 to 1200 MeV/c; K^-d cross sections" (to be published).

APPENDIX I

The neutron detector

The dimensions of this apparatus are those indicated in fig. 3. The detection surface must be of the order of 2 x 2 m^2 in order to cover the whole range of neutron angles for each of the different settings of the magnet (see Appendix II). The minimum neutron momentum in the angular range considered is ~ 300 MeV/c.

The specific set-up is of the type described, for example, in ref. 6. It would consist of a series of spark chambers and scintillators arranged in some 20 modules, each one containing 3 polyethylene plates of 1 cm (so as to have 2 gaps that can be photographed) plus a scintillator plate of 1 cm (to give the signal that the neutron has interacted). Such a system represents approximately 54 g/cm^2 of polyethylene and 21 g/cm^2 of polystyrene (scintillator), i.e. a total of 45 g/cm^2 equivalent of carbon and 9 g/cm^2 of hydrogen. With an imposed minimum range of the recoil proton corresponding to 2 sparks, the overall detection efficiency turns out to be of the order of 30%.

The low rate of triggers expected during the experiment (a maximum of ~ 2 per pulse, with an average of ~ 0.1) does not justify the complication and the added expense of a fast digitizing system. The advantage of the apparatus described are:

1) a low expenditure for the large dimensions required;
2) a good determination of the vertex of the np interaction; the precision will be of the order of $\pm$ 0.5 cm versus the $\pm$ 2.5 cm obtainable with time-of-flight methods;
3) a good rejection on the background of uncorrelated tracks (which will be due mostly to γ-rays);

---

6. L.G. Pondrom et al., University of Wisconsin preprint PPAR 6 (1969).

4) the possibility of obtaining a rough measurement of the neutron polarization from the direction of the recoil proton;

5) the possibility of selecting a subset of elastic np events from which the neutron energy could be measured; thus an additional constraint to the $K^- d \rightarrow K^- n\ (p_s)$ reaction would be available.

The detection efficiency of the apparatus must be determined precisely. For this, we will recur to the differential cross section of the reaction $\pi^- d \rightarrow \pi^- n\ (p_s)$. This reaction can be exactly calibrated because it must be identical to the reaction $\pi^+ p \rightarrow \pi^+ p$ well known throughout the momentum range in question.

APPENDIX II

The Magnet

The magnet would have the general characteristics of the type known at CERN as MNP22A/B; i.e., an opening of 1 m (width) x 0.5 m (height) and a field of 10 KG over a length of 1 m. Referring to the layout of fig. 3, such a magnet has a horizontal acceptance of $\pm 10^{\circ}$ around the angle θ_K of the outgoing K^- (K^-_{out}).

The reaction under study takes place on a moving target, thus an angle of emission θ_K of K_{out} in the laboratory does not correspond to a well determined angle θ_n of the neutron. Instead, there will be a spread of θ_n over an interval which can be calculated from the neutron wave function in the deuteron. Fig. 5 shows the relation between θ_K and θ_n for the two extreme momenta of the region to be explored. The limits indicated by the solid curves on θ_n, for a fixed θ_K, correspond to the angular region where 99% of the recoil neutrons would be found according to the Hulthen distribution. Thus a total of 6 settings (partially overlapping) are necessary to cover most of the angular region. Both the magnet and the neutron detector must be displaced (see fig. 5). As for the very forward direction, it should be noticed that, beyond a certain angle, the measurements lose their meaning as far as K^-n elastic scattering, since there is no way of knowing if the interaction has taken place on the neutron or the proton or both. This limit depends, of course, on the incident momentum and on what can be considered an acceptable probability for the interaction to have taken place on the neutron. Practical considerations (magnet size, dimensions of the chambers, etc.) impose a limit of $\sim 5^{\circ}$ on θ_K. This corresponds to momenta of the recoil neutron which, in the incident momentum region from 1 to 2 GeV/c extend even below the 300 MeV/c value which is customary to take as the lower limit for a K^-n elastic scattering. The value of $\cos \theta^*_K$ in the reaction centre of mass corresponding to a neutron momentum of 300 MeV/c is shown in fig. 6 as a function of the incident K^- momentum. The rates calculated in Appendix III

take into account only the events produced with a cos θ_K^* value smaller than that of fig. 6.

We expect a precision of $\pm$ 1 mm on the intersections of K^-_{out} with the chambers C_1 to C_6 of fig. 3*). Neglecting the effect of multiple scattering, this implies an accuracy on the momentum of K_{out} given by $dP/P = (1.75/300)\sqrt{2}\ P(GeV/c)$; thus at 2 GeV/c, dP/P would be $\sim$ 1.6%.

---

*) We plan to use the multiwire proportional chambers of the type developed at CERN by G. Charpak.

APPENDIX III

Rates and time estimate

As mentioned in Appendix II, the angular region of K_{out} would be covered in 6 steps. It should be pointed out that there is no reason why the different angular regions should be given equal importance. Thus, for example, an accurate measurement of the backward region ($\cos \theta^*_K < 0$) seems more useful than a precise measurement of the forward region where the diffraction peak (if there is such a peak) would mask the presence of the resonant contributions. On the other hand, at present we are not in a position to make an a-priori guess of the relative importance of the various regions. This may well be done at a later stage, when part of the data has been obtained. Thus, for the moment, we have simply apportioned the running time at each setting according to the solid angle in the centre of mass covered by the setting.

Furthermore, for lack of better information, we have used the K^-p elastic scattering cross sections (from ref. 2) as if they pertained to the K^-n reaction. The indications near 1 GeV/c are that the two processes are indeed very similar (see fig. 4).

We then make the following assumptions:

1) the incident K^- flux is that of the m7 beam (thus we take, for example, $\sim$ 5,000 K^- per 10^{12} protons at 1.5 GeV/c with a dP/P of $\pm$ 1%);
2) the proton flux on the internal target is $8 \cdot 10^{11}$ per pulse with 2.7 seconds between pulses;
3) the neutron detector has a 30% efficiency;
4) the overall efficiency in the use of allocated time is 60%.

Under these conditions, we give in fig. 7 the number of elastic K^-n events obtainable in one PS week as a function of the incident K^- momentum. It appears that <u>one</u> week is about the right amount of time

necessary to obtain a satisfactory statistics at one momentum setting. It is true that in this way more statistics would be collected at the higher momenta than at the lower, but this is not unreasonable in view of the increased complexity of the differential cross sections with increasing incident momentum. Furthermore, we should take into account that the spread of the centre of mass energy, due to the Fermi motion of the neutron, distributes the events from the individual momentum settings over a region of ~ 150 MeV/c around the nominal value (~ 2/3 of the events are included in this region). Thus a total of 6 momentum settings, spaced by ~ 150 MeV/c, are sufficient to cover the region from ~ 1.2 to ~ 2.2 GeV/c. Grouping all the events together and re-apportioning them in finer momentum bins would then be done so as to provide the detailed information in the form most convenient to the needs of the partial wave analysis.

Figure Captions

Fig. 1 The status of experiments on K^-p interactions in the momentum region from ~ 1 to ~ 2 GeV/c. As an indication, we show the total, elastic and charge exchange cross sections. The arrows indicate the position of resonances.

Fig. 2 Seventh order coefficients of the expansion of $d\sigma/d\Omega$ and $P\ d\sigma/d\Omega$ defined in the text. The K^-p data are from ref. 2, the $\bar{K}^0n$ from ref. 4. The curves are described in the text.

Fig. 3 Layout of the apparatus. S indicates hodoscopes, C Charpak chambers. The length of the target is 25 cm. (distances are to scale)

Fig. 4 Some differential cross sections of (a) $K^-p \to K^-p$ and (b) $K^-n \to K^-n$ from ref. 5.

Fig. 5 Laboratory angle of the neutron and the outgoing K^-. The dotted curve corresponds to the elastic scattering $K^-n \to K^-n$ if the neutron were at rest in the laboratory. The solid lines indicate the region covered by one of the particles when the other is at a fixed angle. The boxes show the angular regions covered by the different settings of the magnet and the neutron detector.

Fig. 6 Value of $\cos \Theta_K^*$ in the centre of mass of the K^-n system corresponding to a neutron momentum of 300 MeV/c, as a function of the incident K^- momentum. The differential cross section would be measured only up to these values.

Fig. 7 Number of events $K^-n \to K^-n$ obtainable in <u>one</u> PS week at the various momenta between 1 and 2 GeV/c with the conditions specified in the text. Vertical dashed lines indicate the momentum settings of the run.

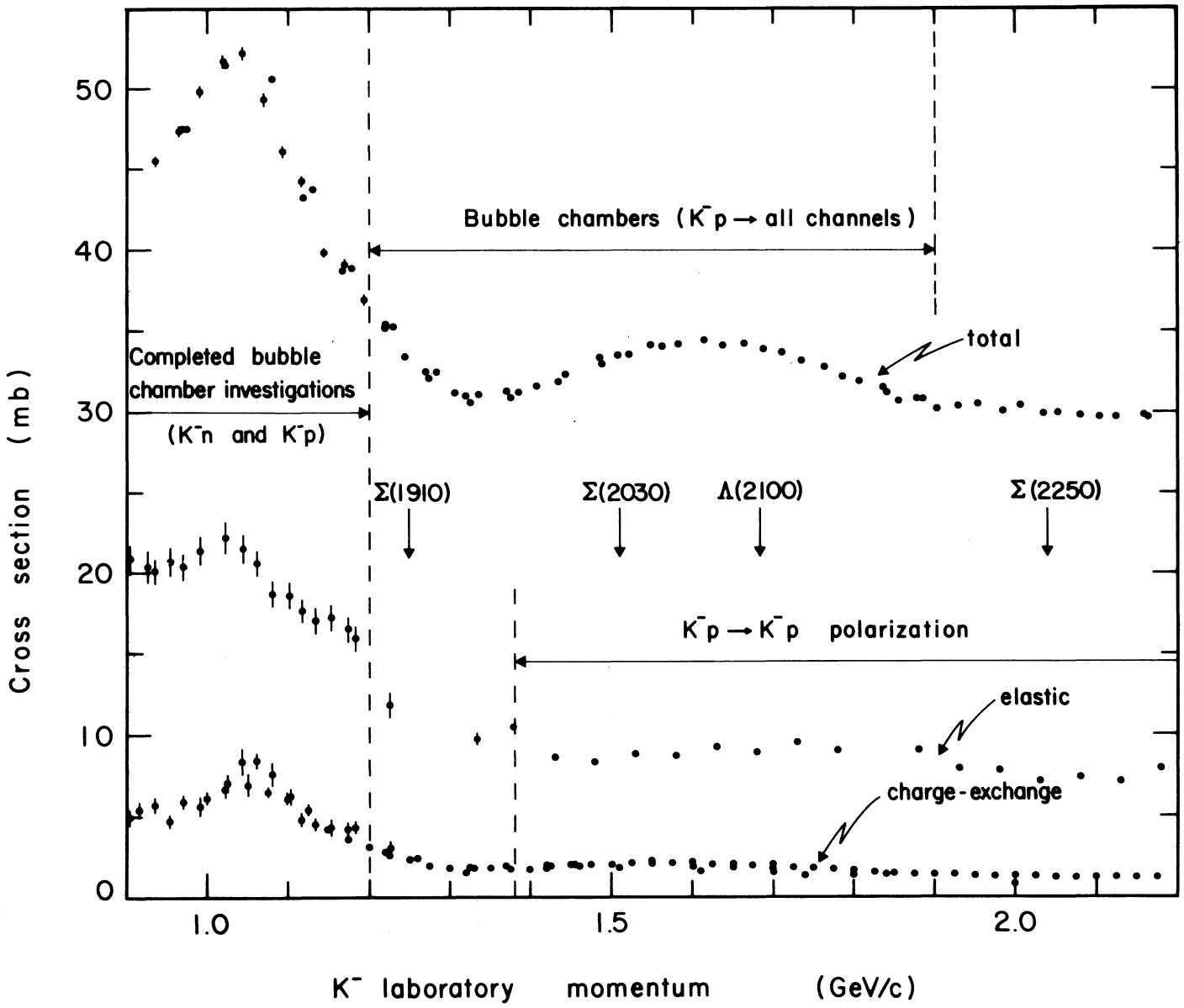
Cross section (mb)
50
40
30
20
10
0
1.0
1.5
2.0
K⁻ laboratory momentum (GeV/c)
Bubble chambers (K⁻p → all channels)
Completed bubble chamber investigations (K⁻n and K⁻p)
total
Σ(1910)
Σ(2030)
Λ(2100)
Σ(2250)
K⁻p → K⁻p polarization
elastic
charge-exchange

Figure I

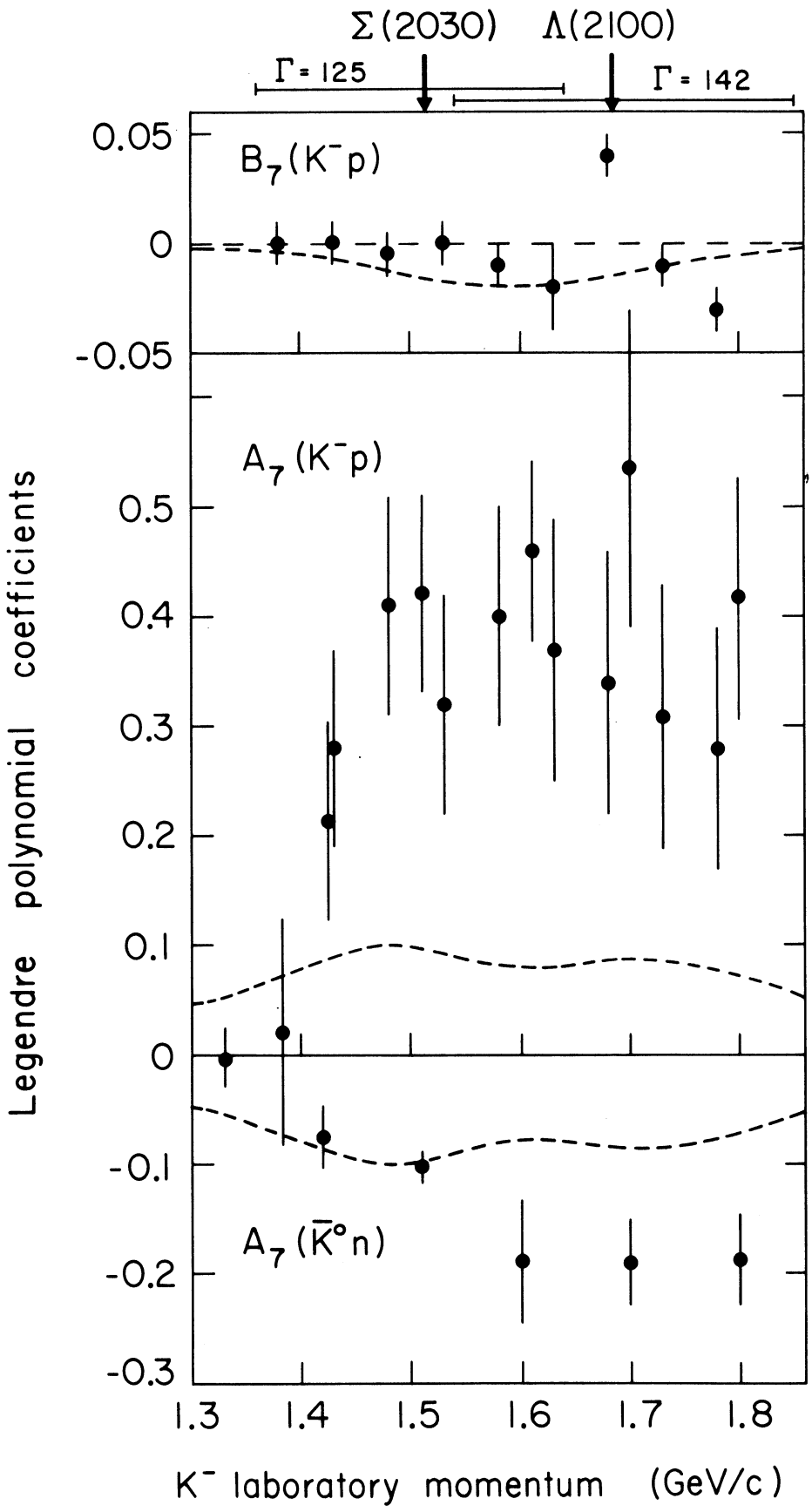
Σ(2030)
Λ(2100)
Γ = 125
Γ = 142
0.05
0
-0.05
$B_7(K^-p)$
$A_7(K^-p)$
0.5
0.4
0.3
0.2
0.1
0
-0.1
$A_7(\bar{K}^0n)$
-0.2
-0.3
1.3
1.4
1.5
1.6
1.7
1.8
Legendre polynomial coefficients
K^- laboratory momentum (GeV/c)

Figure 2

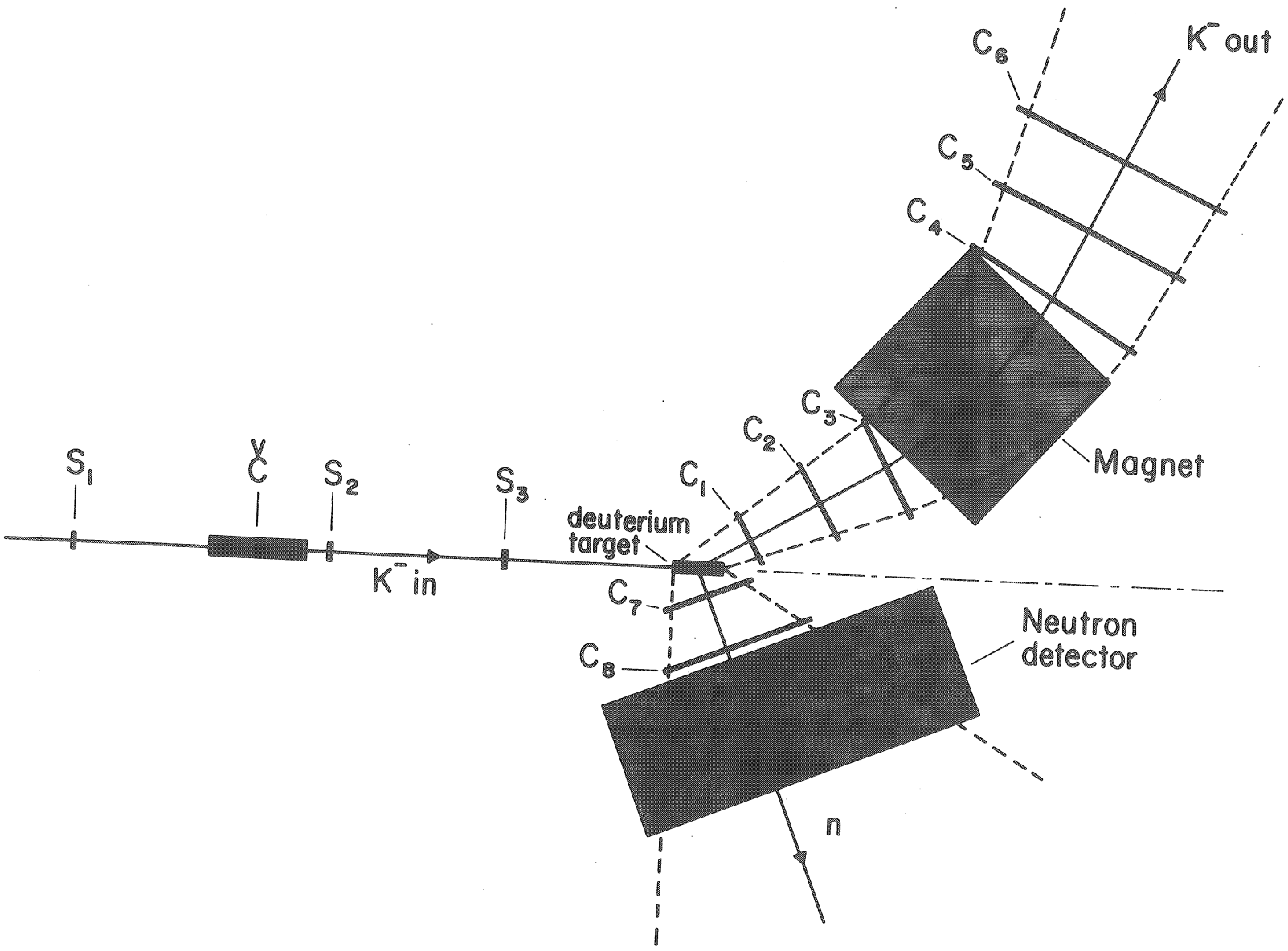
C6
K⁻ out
C5
C4
C3
C2
C1
Magnet
S1
V
C
S2
S3
deuterium
target
K⁻ in
C7
C8
Neutron
detector
n

Figure 3

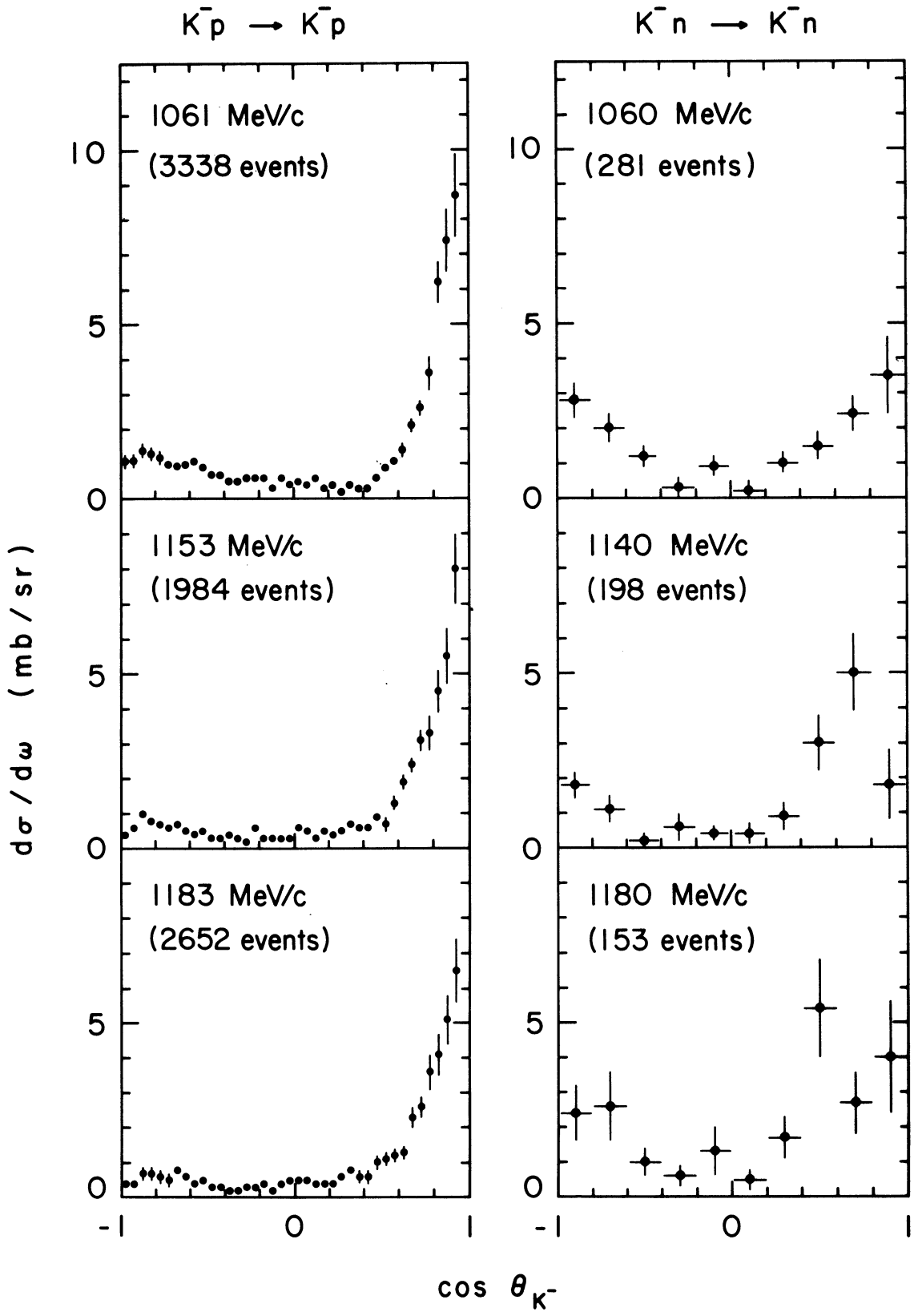
K⁻p → K⁻p
K⁻n → K⁻n
1061 MeV/c
(3338 events)
1060 MeV/c
(281 events)
1153 MeV/c
(1984 events)
1140 MeV/c
(198 events)
1183 MeV/c
(2652 events)
1180 MeV/c
(153 events)
dσ / dω (mb / sr)
cos θ K⁻

Figure 4

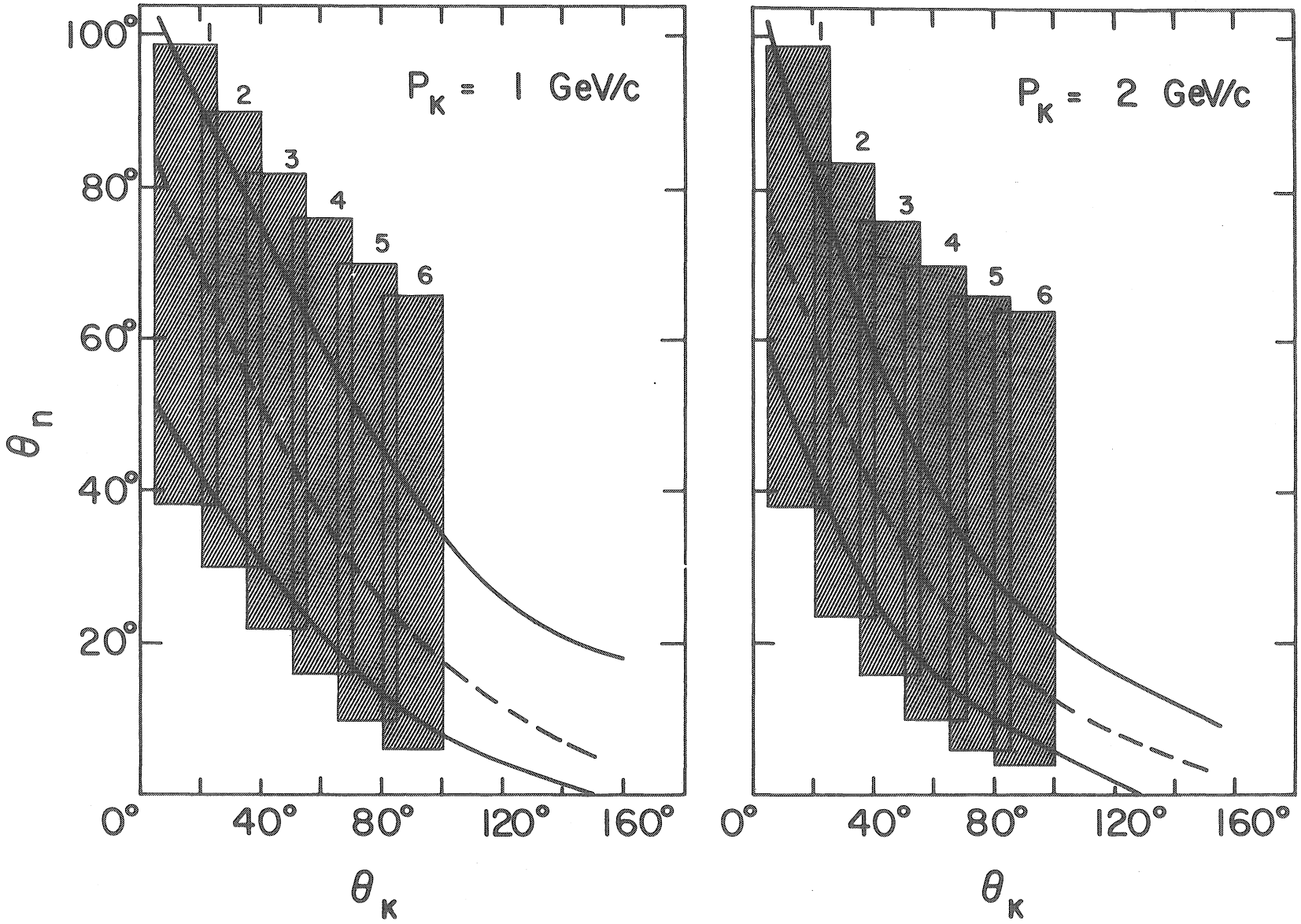
100°
80°
60°
40°
20°
0°
40°
80°
120°
160°
θ_n
θ_K
P_K = 1 GeV/c
P_K = 2 GeV/c
2
3
4
5
6

Figure 5

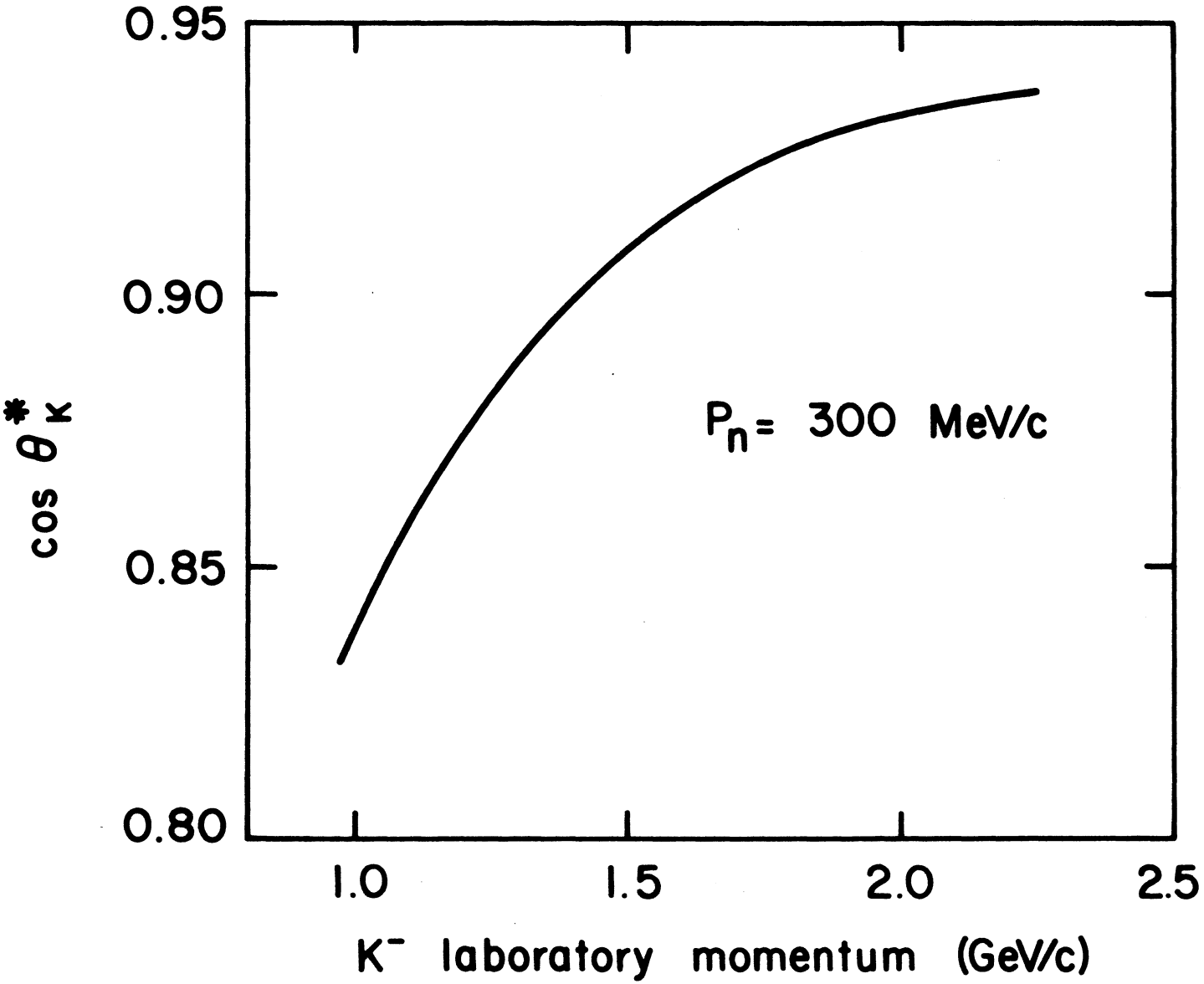
0.95
0.90
0.85
0.80
cos θ*K
P_n = 300 MeV/c
1.0
1.5
2.0
2.5
K⁻ laboratory momentum (GeV/c)

Figure 6

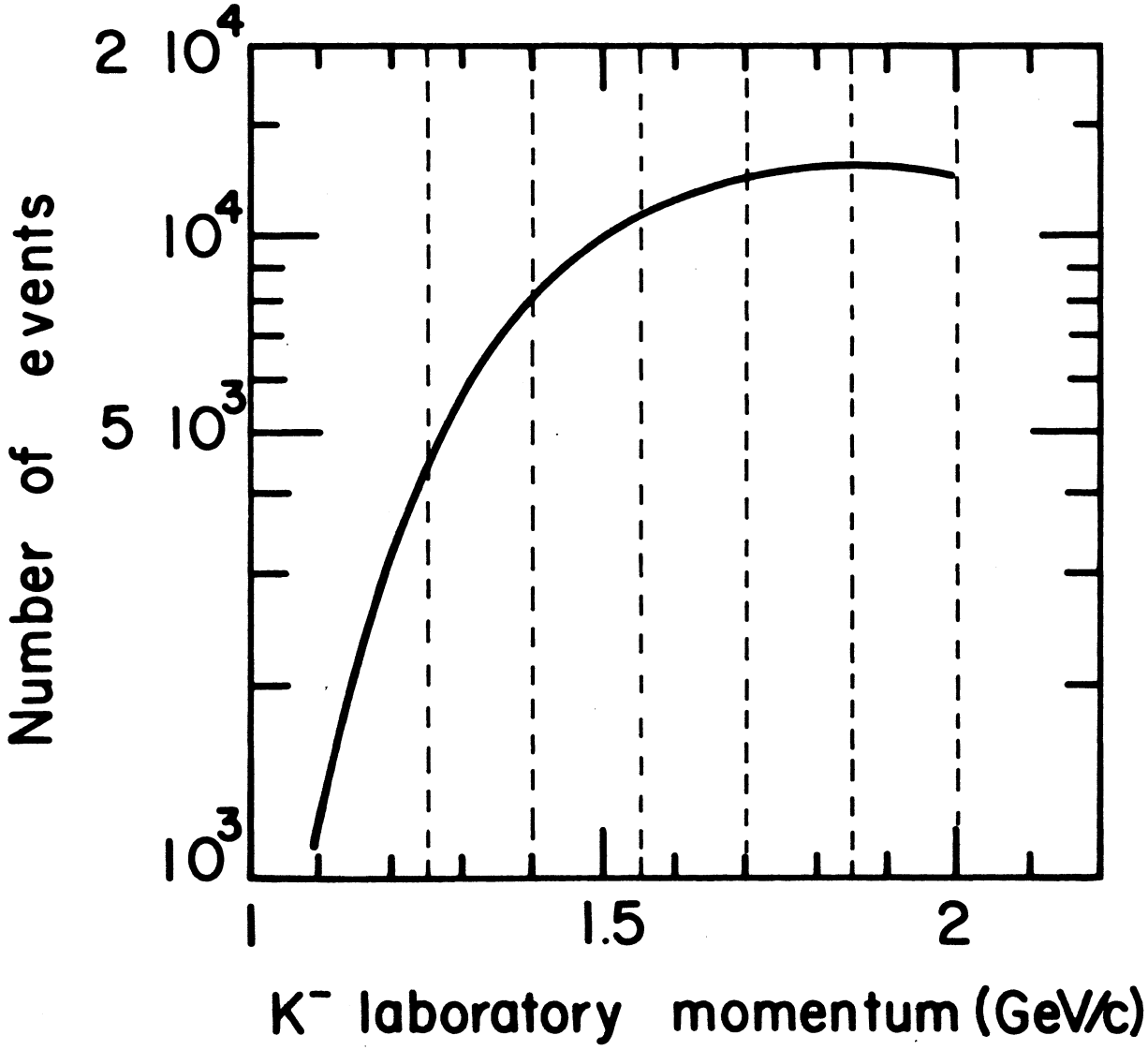
2 10^4
10^4
5 10^3
10^3
Number of events
1
1.5
2
K⁻ laboratory momentum (GeV/c)

Figure 7